Rev. Roum. Sci. Techn.– Électrotechn. et Énerg.
Vol. **70**, *1*, pp. 103–108, Bucarest, 2026

METAHEURISTIC-DRIVEN DUAL INDUCTOR BOOST CONVERTER FOR FLOATING PV SYSTEMS IN MATLAB/SIMULINK

ANBARASU PALANISAMY[1], LOGANATHAN NAVANEETHA KRISHNAN[2], NARENDRAN ARUMUGHAM[3], RAMESHKUMAR KANAGAVEL[4]

Keywords: Dual inductor boost converter (DIBC); Maximum power point tracking (MPPT); Floating photovoltaic (FPV); Improved perturb and observe (IP&O); MATLAB/Simulink.

The best way to present a floating photovoltaic (FPV) system would be to recognize the increasing demand for renewable energy sources and the challenges faced by traditional land-based solar systems, including limited space and the astronomical costs of installation. One of the possible solutions to these problems is FPV systems, which use water surfaces as a place to install solar panels, such as lakes, reservoirs, and ponds. The research paper will help optimize the energy collection process for FPV systems by developing an Improved Perturb and Observe (IP&O) algorithm with a dual-inductor boost converter (DIBC). This is aimed at precise monitoring of the peak power point, particularly under changing environmental conditions. The simulation results of the suggested MPPT approach in MATLAB/Simulink are consistent with those reported in the literature. The findings show that reaction time and overall functionality of the FPV system improved significantly, highlighting the possible benefits of the IP&O algorithm for optimizing the energy output of floating solar arrays compared to the traditional MPPT approach.

1. INTRODUCTION

Energy plays a very crucial role in the development of countries. Over the centuries, fossil fuels have always been the main source of energy in the entire world. However, due to the rapid population increase, improved living standards, and the development of energy-consuming activities in both developed and developing countries, global energy use has increased significantly. Enhanced energy consumption has led to worsening of the global warming problem, where much of this energy consumption is a result of increased emission of greenhouse gases [1].

The global initiative to reduce carbon emissions has awakened a growing interest in carbon-free and cost-efficient renewable energy (RE) technologies, which require proper management and exploitation [2]. Among all the RE sources, solar energy, *i.e.*, solar photovoltaic (SPV), is extremely remarkable. The most common technology is SPV, which has been implemented globally and is cost-effective, and has the potential to reduce power shortages in certain developing nations. According to a report released by the International Renewable Energy Agency, the global renewable energy potential would increase by 50 % by the year 2019 and 2024 with the addition of nearly 1220 GW.

There is a need to maximize the use of solar energy. There has been a significant effort to streamline the design and production of solar cells to improve efficiency and reduce costs [3]. It has been reported that despite some improvements, there is still a need to improve the overall system performance, which is to get maximum power out of PV panels [4]. The most used device for this purpose is the MPPT controller.

The literature [6] offers a thorough examination of several MPPT approaches. Researchers have employed many MPPT methods in a range of investigations. The P&O approach fine-tunes the voltage until it hits the MPP. Although P&O is considered a straightforward method, its conventional variants often display stable oscillations near the MPP. The proposed technique mitigates this issue by limiting the search region to a region close to the MPP [7]. This study presents a developed P&O-based MPPT algorithm that restricts the search space and models a dual inductor boost converter for the FPV system.

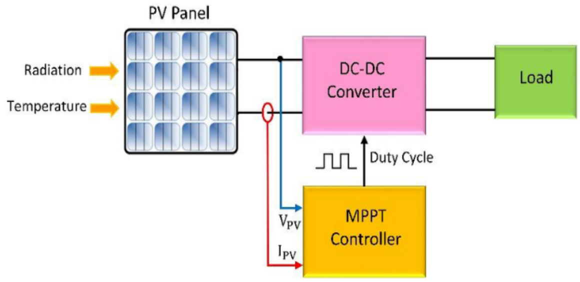

Fig.1 – Typical MPPT with DC/DC converter.

The rest of the paper is organized in the following order. Section 2 describes the components of the floating photovoltaic system. Section 3 gives the modelling of the DIBC converter with MPPT for the FPV system. Section 4 describes the traditional and improved P&O algorithms. Section 5 deals with hardware and software implementation, along with the experimental results. Finally, Section 6 concludes the paper with a future research scope.

2. FLOATING PHOTOVOLTAIC SYSTEM

The FPV systems are a new phenomenon, which is yet to be rolled out commercially, with only a few demonstration projects being rolled out around the world [8]. A lack of space to install traditional PV systems is being witnessed, especially in many places, such as the islands, such as the Philippines, Singapore, Japan, and Korea, thus making FPV systems an option. Floating solar systems can be fitted in many water bodies such as lakes, vineyards, fish farms, dams, canals, irrigation ponds, reservoirs, seas, and lagoons. An average PV module can convert 4 to 17 % of the amount of solar energy it obtains into electricity. The remaining solar energy is converted into thermal energy, thus leading to a significant rise in temperature of the PV modules [9]. Temperature variations have a direct influence on the efficiency of solar cells by disturbing their power output. The solar PV installation on water surfaces is advantageous due to the cooling action of water, which leads to a notable decrease in the surrounding temperature [10]. Utilizing aluminium frames to uphold the floating solar PV modules facilitates the transmission of lower temperatures from the water, hence further diminishing the overall module's temperatures. Floating solar panels exhibit an average efficiency that exceeds ground-mounted solar panels by 11% [11]. The FPV system comprises

[1] Department of EEE, Sri Eshwar College of Engineering, India. Email: anbarasu.p@sece.ac.in
[2] Department of EEE, Sri Krishna College of Engineering and Technology, India. Email: loganathann@skcet.ac.in
[3] Department of EEE, SRM Madurai College for Engineering and Technology, India. Email: narendran@srmmcet.edu.in
[4] Department of EEE, Dr. Mahalingam College of Engineering and Technology, India. Email: rameshkumar@drmcet.ac.in

DOI: 10.59277/RRST-EE.2026.1.17

pontoons or individual floats, solar panels, a mooring system, and cables, as seen in Fig. 2.

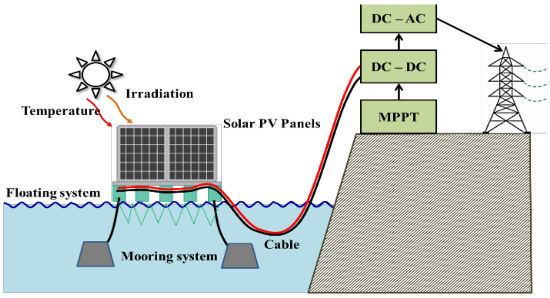

Fig. 2 – FPV system architecture.

3. MODELLING OF DIBC WITH MPPT FOR FPV SYSTEM

3.1 SOLAR PHOTOVOLTAIC (SPV) CELL

SPV cells are semiconductor devices that generate electrical energy from solar radiation. The temperature, the intensity of the sun's rays, and the fundamental characteristics of the solar cell material all affect its effectiveness [12]. The PV cell's electrical equivalent circuit is displayed in Fig. 3.

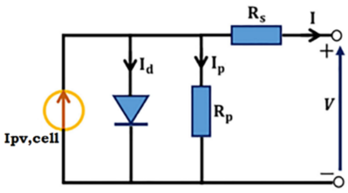

Fig. 3 – SPV equivalent circuit.

For the above PV model, a current source ($I_{pv,cell}$) is considered, along with a reverse diode, series resistance R_s, and parallel resistance R_p. The output current from the ideal PV cell is as follows [13]

$$I = I_{pv,cell} - I_{o,cell}\left[\exp\left(\frac{qV}{akT}\right) - 1\right], \tag{1}$$

where, $I_{pv,cell}$ is the current generated by incident light [A], $I_{o,cell}$ is the reverse saturation current of diode [A], q is the electron charge [1.6 x10^{-19} C], k is Boltzmann constant [1.38 x 10^{-23} J/ K], T is the PN junction temperature [K], a is the diode ideality constant [$1 \leq a \leq 1.5$], V is the terminal voltage of the PV Cell [V].

For practical arrays, the basic equation should be modified to account for additional factors to observe the characteristics at the array's terminals. Thus, the output current of the PV cell is expressed as [14],

$$I = I_{pv} - I_o\left[\exp\left(\frac{V + R_s I}{V_t a}\right) - 1\right] - \frac{V + R_s I}{R_p}, \tag{2}$$

where R_s is the series resistance, R_p is the parallel resistance, V_t is the thermal voltage, V is the terminal voltage, and a is the ideality factor.

3.2 DUAL INDUCTOR BOOST CONVERTER (DIBC)

A dual inductor boost converter (DIBC) circuit is a circuit that is used in power conversion between DC and DC. It boosts the DC voltage input source to a greater DC voltage output [15]. The architecture uses two inductors to perform the voltage transformation, which is associated with numerous valuable advantages, such as high efficiency, less voltage stress on the components, and reduced electromagnetic interference (EMI) [16]. The basic operation of this converter involves the input voltage source labeled as V_s, two inductors named L_1 and L_2, and one switch M_s, a MOSFET [17].

The conversion of the energy between L_1 to L_2 helps in the transfer of power to the output capacitor, therefore increasing the output voltage [18]. Nonetheless, to realize the targeted results with this system, a high level of control, selective choice, and component design is needed. Figure 4 above illustrates the DIBC that operates in either of the two modes during operation in continuous conduction mode (CCM); the mode of operation depends on whether the main switch 'Ms' will operate in Mode I or Mode II.

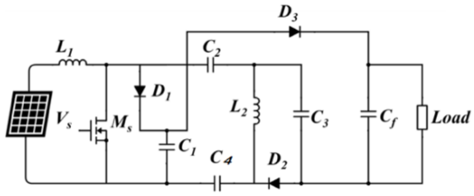

Fig. 4 – DIBC configuration.

The converter's linearized small-signal state-space averaged model is represented by equation (3) [19].

$$\begin{bmatrix} V_c' \\ I_L' \end{bmatrix} = \begin{bmatrix} \frac{(1-D)}{C} & -\frac{1}{C.R_L} \\ 0 & -\frac{(1-D)}{L} \end{bmatrix} \begin{bmatrix} I_L \\ V_C \end{bmatrix} + \begin{bmatrix} 0 \\ \frac{V_C}{L} \end{bmatrix} D, \tag{3}$$

where R_L is the load resistance, D is the duty cycle, V_C is the capacitor voltage, I_L is the inductor current, C, L is the filter capacitor and inductor, respectively.

Consequently, eq. (4) describes the transfer function model of DIBC boost mode with the voltage control model [19].

$$\frac{V_c'}{D} = \frac{V_C}{C.L} * \left(\frac{1-D}{s^2 + \frac{s}{R_L.C} + \frac{(1-D)^2}{LC}}\right) \tag{4}$$

where, V_c' is the enhanced output capacitor voltage, s is the frequency domain element, $s = j\omega = j2\pi f_s$

3.3 DESIGN OF DIBC WITH FPV SYSTEM

In the present study, a polycrystalline solar panel whose Vm and Im were 38.73 V and 8.40 A, respectively, was used by procuring the panel through an FPV system. Through the empirical study, it is realized that the photovoltaic module produces a difference of electrical potential between 27 V and 32 V, which is prone to changing with ambient temperature and solar radiance [20]. The choice of converter elements is made with the aim of reaching a 300 V output for the conversion of DC to AC. Here, the values of converter components that are used in design are discussed [21]. The design parameters are shown in Table 1 to ensure that the proposed DIBC is correct.

Table 1

Design of the proposed DIBC.

Parameters	Value
Output Voltage (V_o)	300 V
Maximum Input Voltage (V_{max})	200 V
Minimum Input Voltage (V_{min})	180 V
Inductors (L_1 & L_2)	694 μH
Switching Frequency (fs)	20 kHz
Filter Capacitor (C_f)	2200 μF
Capacitors (C_1 , C_2 & C_3)	1200 μF
Minimum Duty Cycle (% D_{min})	33.3 %
Maximum Duty Cycle (% D_{max})	40 %

4. **MPPT ALGORITHMS**

The Efficient energy generation in FPV systems is a crucial task that relies largely on the effective utilization of conventional MPPT algorithms.

4.1 TRADITIONAL P&O ALGORITHM

The standard P&O approach is normally used due to its simplicity in implementation, as observed in the flowchart in Fig. 5. This is an iterative method of tracking and adjusting the operating point until it gets to the MPP [22]. This can be done by comparing voltages and power at time (K) with those at the last sample time (K-1) to predict the approach to the MPP. Even a small change in voltage can alter the solar panel's power output [23]. To have a positive power change, the direction remains constant in voltage. When a change of negative power occurs, the MPP moves further to the right, and the perturbation decreases to move towards the MPP. In this process, one checks the entire PV curve with minor adjustments to find MPP, therefore, improving the reaction time of the algorithm [24–27]. However, at high perturbation size, one will encounter repeated oscillations on the MPP.

4.2 IMPROVED IP&O MPPT

The issues that have been identified in the conventional methodology can be addressed through the proposed changes. The new approach limits the exploration range to only 10% of the power curve, which leads to a reduction in the response time and a reduction in sustained oscillations. The literature states that the maximum power point voltage (VMPP) is estimated to be 76% of the open circuit voltage (VOC) as shown in the literature [28]. Such a division of the P-V curve makes three distinct regions clearly defined. Figure 6: Area 1, Area 2, and Area 3. The search zone does not include areas 1 and 3, which form about 90 percent of the power curve. The maximum limit of the MPP is confined to area 2, which covers the MPP. The algorithm proposed does not aim at optimizing the power point in Areas 3 and 4, which would increase efficiency and stability. The flowchart of the IP&O is presented in Fig. 7 [29]. Initially, it detects the voltages V_1 and V_2 to identify the region where the MPP is located and restricts the solar panel's operating point to Area 2.

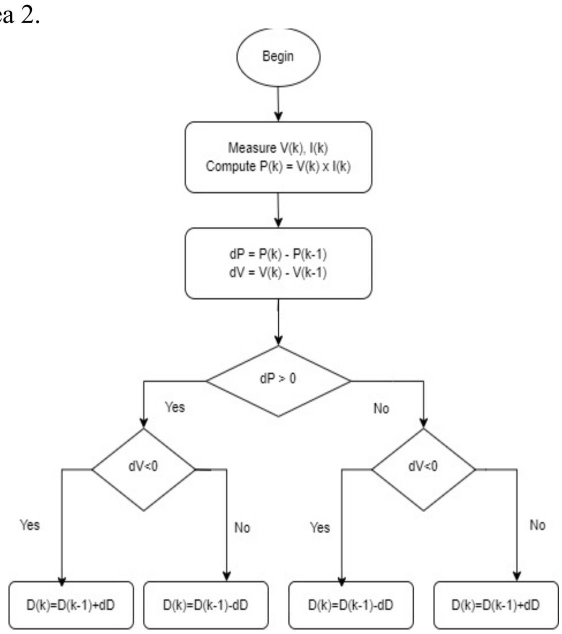

Fig. 5 – Flowchart of traditional P&O algorithm

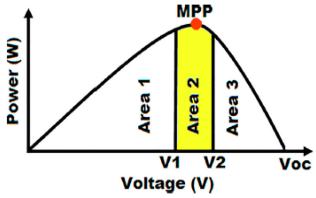

Fig. 6 – Search space for IP&O algorithm.

The MPPT's objective is to expand the performance of solar panels by ensuring they consistently function at their highest power output, regardless of fluctuations in weather conditions and shade [30].

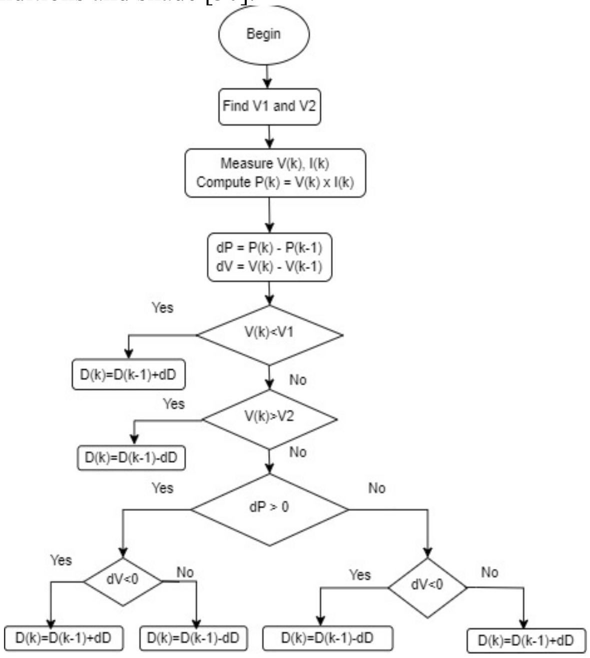

Fig. 7 – Process flow diagram of IP&O algorithm.

5. **RESULTS AND DISCUSSION**

5.1 HARDWARE IMPLEMENTATION

The reservoir is in kondampatti, Tamil Nadu (South India).

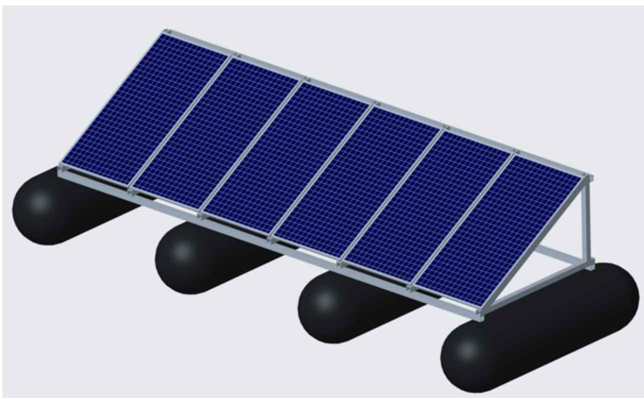

Fig. 8 (a) – Isometric view of the installed FPV system site.

The FPV system has an area of 29 m^2 (20% of the reservoir water surface area) corresponding to a maximum installed capacity of 2 kW. The experimental setup is composed of a polycrystalline PV 330 Wp panel of 6 numbers with 4 pontoons, as shown in Fig. 8 (a). The assembled setup front view is shown in Fig. 8 (b).

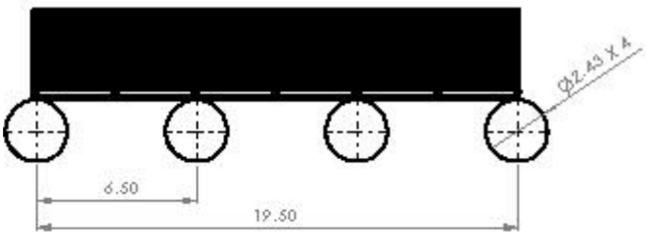

Fig. 8 (b) – Assembled Setup Front view

ripple, which is 2.5 V and 1.25 A during 4.9995 to 5.0005 ms respectively.

The output current and voltage waveforms of DIBC with the IP&O algorithm during 0 to 10 ms are presented in Fig. 11 (a). The ripple voltage of the converter during 4.9995 to 5.0005 ms is about 2.2 V, and the current ripple is found as 0.1 A, as illustrated in Fig. 11 (b). The proposed system with IP&O MPPT method reduces the peak magnitude (12%), peak overshoot (70%), settling time (23%), peak time (7%)

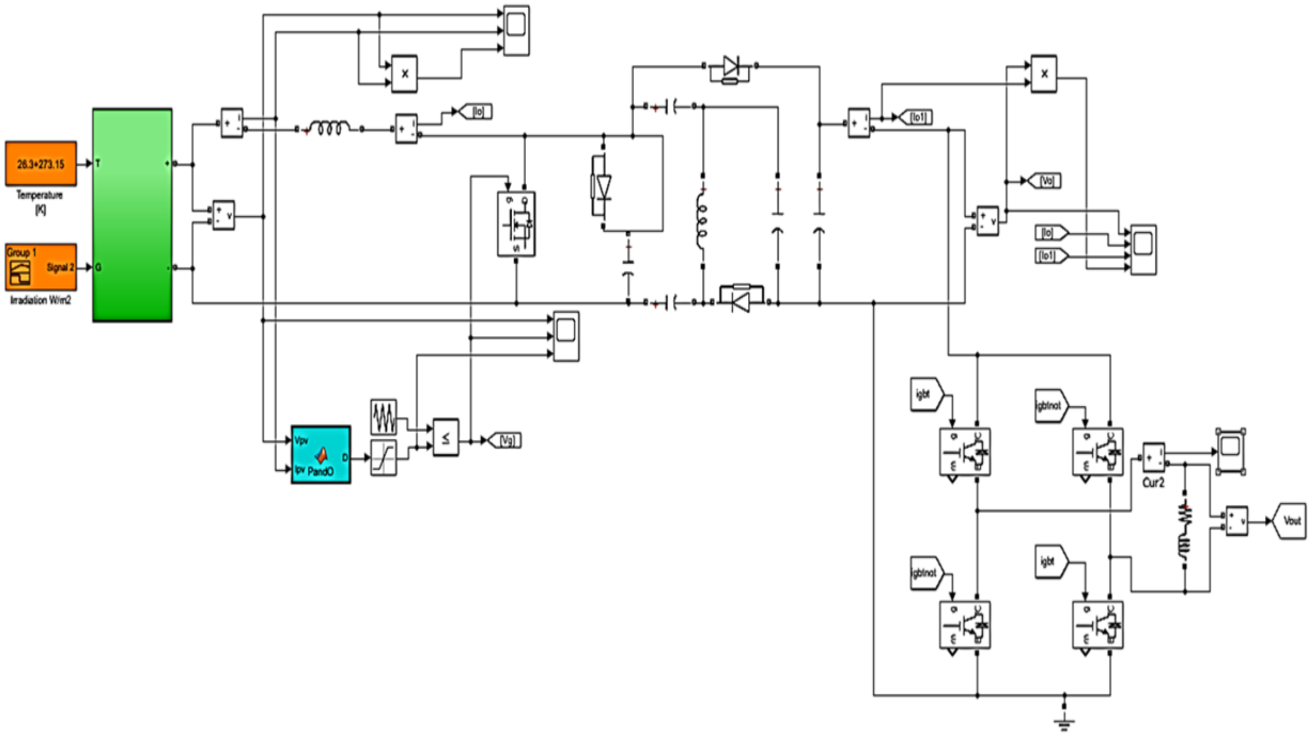

Fig. 9 – MATLAB/Simulink model of FPV system with DIBC.

Specifications of PV panel under standard test conditions are as follows: PV panel has 72 cells, maximum voltage is 35.62 V, maximum current is 6.90 A, maximum power is 245.88 W, Voc is 42.85 V, Isc is 7.29. The weight of each panel is 20.5 kg, MC4 connector is used to connect the PV panels together.

5.2 SOFTWARE IMPLEMENTATION

The modeling of DIBC for the FPV system presented in the previous section is used to develop a Simulink model for the preferred output and input values. Fig. 9 illustrates the proposed FPV system with the DIBC using MATLAB/SIMULINK environment.

The DIBC transfer function model is predicted for the desired input and output requirements as follows [19],

$$T(s)=\frac{349.2}{4.286\text{e-}06\ s^2 + 0.001948\ s + 1}. \qquad (32)$$

To examine the step response, one must introduce a step change in V_s and then monitor the step response of V_o. The behaviour of the step response is contingent upon the overall presentation of the control system, which encompasses both the controller and the feedback loop.

The current waveforms and input voltage of DIBC with IP&O is shown in Fig. 10 (a) and the irradiation and temperature of the FPV is varied during 5 ms and the corresponding Vin variation is shifted from 180 V to 200 V. Figure 10(b) illustrates the DIBC's voltage and the current

and rise time (5%) than conventional P&O method as shown in Fig. 12. Thus IP&O based MPPT system is more efficient for FPV system.

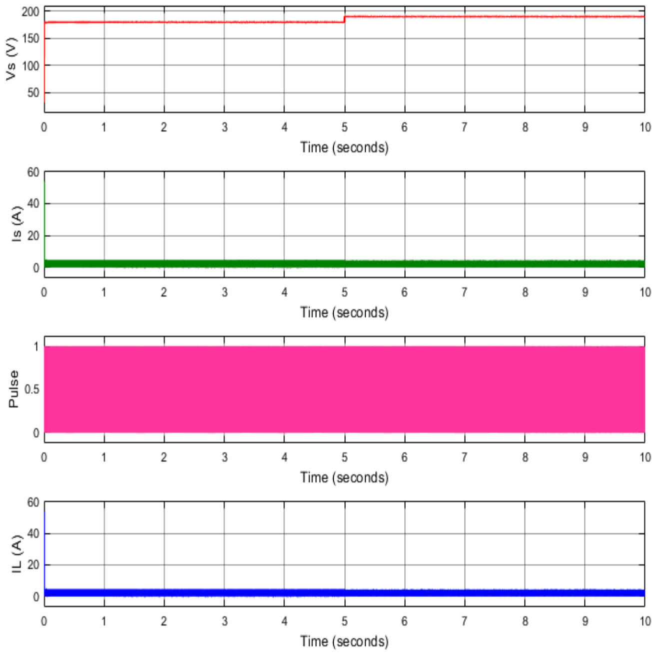

(a)

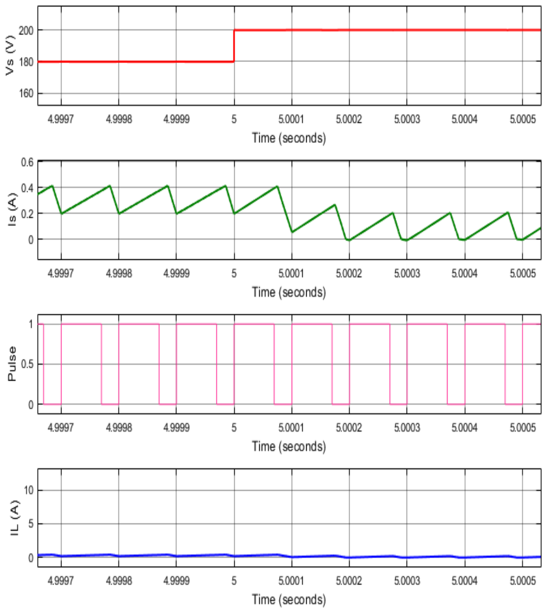

(b)

Fig. 10 – Input voltage and current waveforms of DIBC with IP&O: (a) During 0-10 ms; (b) Ripple values during 4.9995 to 5.0005 ms.

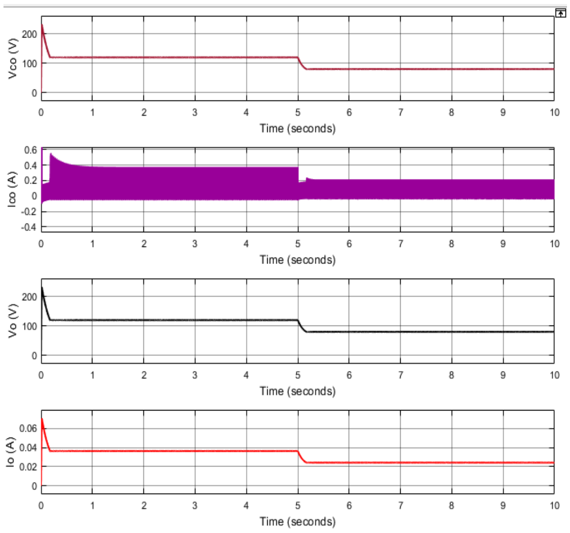

(a)

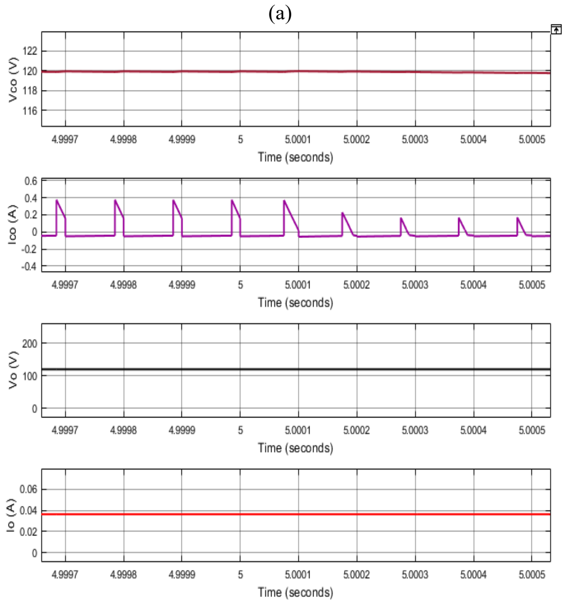

(b)

Fig. 11 – Output voltage and current waveforms of DIBC with IP&O: (a) During 0-10 ms; (b) Ripple values during 4.9995 to 5.0005 ms.

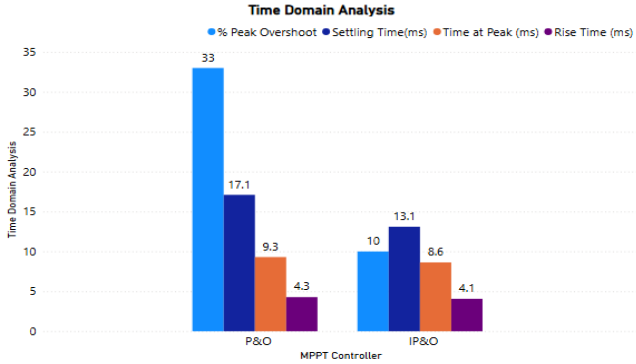

Fig. 12 – Comparison of DIBC performance with MPPT controller system.

6. CONCLUSION

An approach for DIBC has been created to boost FPV system effectiveness. The efficiency of an FPV system is a crucial measure of its performance, which may be improved by employing different MPPT approaches to optimize power production. This is particularly important when dealing with unexpected weather conditions. The time domain analysis of the proposed MPPT and traditional P&O algorithms is compared and studied to enrich the performance of FPV systems. The proposed technique improves upon the standard approach, resulting in reduced complications and improved performance in both stable and variable weather circumstances. The IP&O algorithm improves the step responsiveness and eliminates steady-state oscillations around the MPP, making it superior to the standard technique for FPV systems.

The future study can be the combination of a predictive controller based on artificial intelligence to achieve a superior dynamic response to extreme environmental conditions.

ACKNOWLEDGEMENT

The author would like to thank Sri Eshwar College of Engineering, Tamil Nadu, India, for providing funds and laboratory facilities to carry out the research work.

CREDIT AUTHORSHIP CONTRIBUTION STATEMENT

Anbarasu P: Investigation, Project administration, Writing original draft
Loganathan N: Software
Narendran A: Validation
Rameshkumar K: Visualization

Received on 17 April 2025

REFERENCES

1. S. Amirtharaj, N.R. Prabha, *Cloud service and SCADA-based web application for monitoring renewable energy systems*, Rev. Roum. Sci. Techn. – Électrotechn. et Énerg., **70**, *1*, pp. 57–62 (2025).
2. B. Gopinath, S. Suresh, G. Jayabaskaran, M. Geetha, *Renewable energy resource integrated multilevel inverter using evolutionary algorithms*, Automatika, **65**, *3*, pp. 1061–1078 (2024).
3. J.A. Gotmare, S.V. Prayagi, *Enhancing the performance of photovoltaic panels by stationary cooling*, International Journal of Science, Engineering and Technology, **2**, *7*, pp. 1465–1468 (2014).
4. P. Choudhary, R.K. Srivastava, *Sustainability perspectives—a review for solar photovoltaic trends and growth opportunities*, Journal of Cleaner Production, **227**, pp. 589–612 (2019).
5. L. Khettache, M.R. Rezoug, A. Saadi, L. Sahraoui, *A novel design of a photovoltaic system based on a linear induction motor and reciprocating pump*, Rev. Roum. Sci. Techn. – Électrotechn. et Énerg., **70**, *1*, pp. 3–8 (2025).

6. P.G. Nikhil, M. Premalatha, *Performance enhancement of solar module by cooling: an experimental investigation*, International Journal of Energy and Environment, **3**, *1*, pp. 73–82 (2012).
7. N.L. Devarajan, N.S. Chellathurai, *Aquila optimized nonlinear control for DC-DC boost converter with constant power load*, Rev. Roum. Sci. Techn. – Électrotechn. et Énerg., **69**, *4*, pp. 419–424 (2024).
8. R.S. Kumar, *Performance analysis of polycrystalline floating photovoltaic array: the concept and prototype development for irrigation purpose*, Progress in Photovoltaics, **31**, pp. 738–749 (2023).
9. K. Trapani, D.L. Millar, H.C.M. Smith, *Novel offshore application of photovoltaic in comparison to conventional marine renewable energy technologies*, Renewable Energy, **50**, pp. 879–888 (2013).
10. S. Dubey, J.N. Sarvaiya, B. Seshadri, *Temperature dependent photovoltaic (PV) efficiency and its effect on PV production in the world a review*, Energy Procedia, **33**, pp. 311–321 (2013).
11. M. Syahriman, M. Azmi, M.Y.H. Othman, M.H.H. Ruslan, K. Sopian, Z.A. Abdul Majid, *Study on electrical power output of floating photovoltaic and conventional photovoltaic*, AIP Conference Proceedings, **1571**, pp. 95–102 (2013).
12. S. Motahhir, A. El Hammoumi, A. El Ghzizal, *The most used MPPT algorithms: review and the suitable low-cost embedded board for each algorithm*, Journal of Cleaner Production, **246** (2020).
13. Y. Sahu, M. Shahabuddin, P. Agrawal, *Floating solar photovoltaic system: an emerging technology*, NSPCEP II (2015).
14. H. Yousuf, M.Q. Khokhar, M.A. Zahid, J. Kim, Y. Kim, E.C. Cho, Y.H. Cho, J. Yi, *A review on floating photovoltaic technology (FPVT)*, Current Photovoltaic Research, **8**, *3*, pp. 67–78 (2020).
15. A. Sahu, N. Yadav, K. Sudhakar, *Floating photovoltaic power plant: a review*, Renewable and Sustainable Energy Reviews, **66**, pp. 815–824 (2016).
16. P. Ranjbaran, H. Yousefi, G.B. Gharehpetian, F.R. Astaraei, *A review on floating photovoltaic (FPV) power generation units*, Renewable and Sustainable Energy Reviews, **110**, pp. 332–347 (2019).
17. A. El Hammoumi, S. Motahhir, A. Chalh, A. El Ghzizal, A. Derouich, *Real-time virtual instrumentation of Arduino and LabVIEW based PV panel characteristics*, IOP Conference Series: Earth and Environmental Science, **161**, *1* (2018).
18. B. Aljafari, G. Devarajan, S. Subramani, S. Vairavasundaram, *Intelligent RBF-fuzzy controller based non-isolated DC-DC multi-port converter for renewable energy applications*, Sustainability, **15**, *12*, 9425 (2023).
19. T. Vysagh, K. Sundaramoorthy, *Application of non-isolated quadratic boost DC-DC converter for solar PV integration*, IEEE 19th India Council International Conference (INDICON), pp. 1–5 (2022).
20. F.M. Shahir, E. Babaei, M. Farsadi, *Extended topology for a boost DC–DC converter*, IEEE Transactions on Power Electronics, **34**, *3*, pp. 2375–2384 (2018).
21. A. Rajaei, R. Khazan, M. Mahmoudian, M. Mardaneh, M. Gitizadeh, *A dual inductor high step-up DC/DC converter based on the Cockcroft–Walton multiplier*, IEEE Transactions on Power Electronics, **33**, *11* (2018).
22. N. Hata, N. Belhaouchet, S. Sayah, *Design and experimental validation of an efficient control based on variable step size P&O MPPT technique and predictive current controller for a single-phase grid-connected photovoltaic system*, Electrical Engineering, **105**, pp. 2637–2652 (2023).
23. M.L. Azad et al., *P&O algorithm based MPPT technique for solar PV system under different weather conditions*, 2017 International Conference on Circuits, Power and Computing Technologies (ICCPCT) (2017).
24. S. Salman, X. Ai, Z. Wu, *Design of a P&O algorithm based MPPT charge controller for a stand-alone 200 W PV system*, Protection and Control of Modern Power Systems, **3**, 25 (2018).
25. S. Manna, A.K. Akella, *Comparative analysis of various P&O MPPT algorithm for PV system under varying radiation condition*, 1st International Conference on Power Electronics and Energy (ICPEE), Bhubaneswar, India, pp. 1–6 (2021).
26. S. Ghosh, T.K. Saha, *Progressive step maximum power tracker for cascaded inverter induction motor drive*, Rev. Roum. Sci. Techn. – Électrotechn. et Énerg., **69**, *1*, pp. 3–8 (2024).
27. P. Sharma, B. Muni, D. Sen, *Design parameters of 10 KW floating solar power plant*, IARJSET (2015).
28. D.S. Reddy, *Review on power electronic boost converters*, Australian Journal of Electrical and Electronics Engineering, **18**, *3*, pp. 127–137 (2021).
29. P.K. Dash, N.C. Gupta, *Effect of temperature on power output from different commercially available photovoltaic modules*, International Journal of Engineering Research and Applications, **5**, *1*, pp. 148–151 (2015).
30. M.I. Abdelwanis, A.A. Zaky, *Maximum power point tracking in a perovskite solar pumping system with a six-phase induction motor*, Rev. Roum. Sci. Techn. – Électrotechn. et Énerg., **69**, *1*, pp. 15–20 (2024).